2010 American Control Conference
Marriott Waterfront, Baltimore, MD, USA
June 30-July 02, 2010

Sequential and Iterative Architectures for Distributed Model Predictive Control of Nonlinear Process Systems. Part II: Application to a Catalytic Alkylation of Benzene Process

Jinfeng Liu, Xianzhong Chen, David Muñoz de la Peña and Panagiotis D. Christofides

Abstract— **In the first part of this work [1], we present two different architectures for distributed model predictive control (DMPC) of nonlinear process systems: sequential distributed model predictive control and iterative distributed model predictive control. In the present work, we focus on the application of the theoretical results developed in [1] to a catalytic alkylation of benzene process example, which consists of four continuous stirred tank reactors and a flash separator. In order to carry out the simulations, a first principle model is developed via mass and energy balances. Based on the process model, three distributed Lyapunov-based model predictive controllers are designed to control the process in a coordinative fashion. Extensive simulations are carried out to compare the DMPC architectures proposed in [1] with an existing centralized Lyapunov-based model predictive control design from computational time and closed-loop performance points of view.**

I. Description of the alkylation of benzene process

The process of alkylation of benzene with ethylene to produce ethylbenzene is widely used in the petrochemical industry. Dehydration of the product produces styrene, which is the precursor to polystyrene and many copolymers. Over the last two decades, several methods and simulation results of alkylation of benzene with catalysts have been reported in the literature. The process model developed in this section is based on these references [2], [3], [4], [5], [6]. More specifically, the process considered in this work consists of four continuously stirred tank reactors (CSTRs) and a flash tank separator, as shown in Fig. 1. The CSTR-1, CSTR-2 and CSTR-3 are in series and involve the alkylation of benzene with ethylene. Pure benzene is fed from stream F_1 and pure ethylene is fed from streams F_2, F_4 and F_6. Two catalytic reactions take place in CSTR-1, CSTR-2 and CSTR-3. Benzene (A) reacts with ethylene (B) and produces the required product ethylbenzene (C) (reaction 1); ethylbenzene can further react with ethylene to form 1,3-diethylbenzene (D) (reaction 2) which is the byproduct. The effluent of CSTR-3, including the products and leftover reactants, is fed to a flash tank separator, in which most of benzene is separated overhead by vaporization and condensation techniques and recycled back to the plant and the bottom product stream is removed. A portion of the recycle stream F_{r2} is fed back to CSTR-1 and another portion of the recycle stream F_{r1} is fed to CSTR-4 together with an additional feed stream F_{10} which contains 1,3-diethylbenzene from further distillation process that we do not consider in this example. In CSTR-4, both reaction 2 and catalyzed transalkylation reaction in which 1,3-diethylbenzene reacts with benzene to produce ethylbenzene (reaction 3) take place. All chemicals left from CSTR-4 eventually pass into the separator. All the materials in the reactions are in liquid phase due to high pressure. The dynamic equations describing the behavior of the process, obtained through material and energy balances under standard modeling assumptions, are shown below:

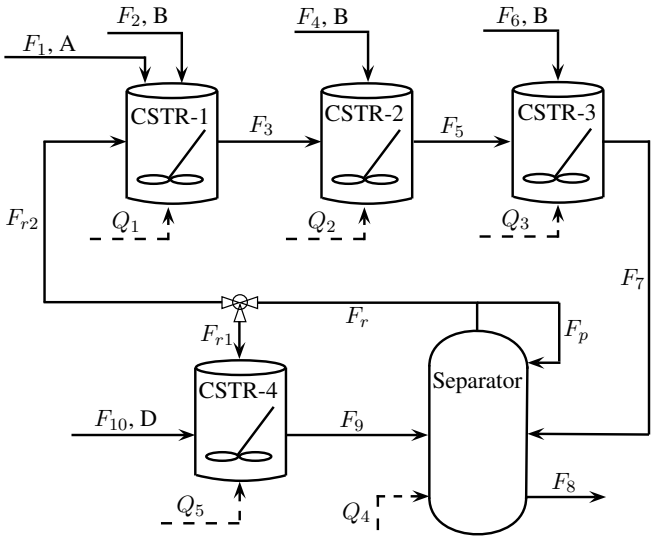

Fig. 1. Process flow diagram of alkylation of benzene.

$$\frac{dC_{A1}}{dt} = \frac{F_1 C_{A0} + F_{r2} C_{Ar} - F_3 C_{A1}}{V_1} - r_1(T_1, C_{A1}, C_{B1}) \quad (1a)$$

$$\frac{dC_{B1}}{dt} = \frac{F_2 C_{B0} + F_{r2} C_{Br} - F_3 C_{B1}}{V_1} - r_1(T_1, C_{A1}, C_{B1}) - r_2(T_1, C_{B1}, C_{C1}) \quad (1b)$$

$$\frac{dC_{C1}}{dt} = \frac{F_{r2} C_{Cr} - F_3 C_{C1}}{V_1} + r_1(T_1, C_{A1}, C_{B1}) - r_2(T_1, C_{B1}, C_{C1}) \quad (1c)$$

$$\frac{dC_{D1}}{dt} = \frac{F_{r2} C_{Dr} - F_3 C_{D1}}{V_1} + r_2(T_1, C_{B1}, C_{C1}) \quad (1d)$$

Financial support from NSF and European Commission, INFSOICT-223866, is gratefully acknowledged.

Jinfeng Liu, Xianzhong Chen and Panagiotis D. Christofides are with the Department of Chemical and Biomolecular Engineering, University of California, Los Angeles, CA 90095-1592, USA. Panagiotis D. Christofides is also with the Department of Electrical Engineering, University of California, Los Angeles, CA 90095-1592, USA, jinfeng@ucla.edu, xianzhongchen@gmail.com, pdc@seas.ucla.edu.

David Muñoz de la Peña is with the Departamento de Ingeniería de Sistemas y Automática Universidad de Sevilla, Sevilla 41092, Spain, dmunoz@us.es.

$$\frac{dT_1}{dt} = \frac{Q_1 + F_1 C_{A0} H_A(T_{A0}) + F_2 C_{B0} H_B(T_{B0})}{\sum_i^{A,B,C,D} C_{i1} C_{pi} V_1} + \frac{\sum_i^{A,B,C,D} (F_{r2} C_{ir} H_i(T_4) - F_3 C_{i1} H_i(T_1))}{\sum_i^{A,B,C,D} C_{i1} C_{pi} V_1} + \frac{-\Delta H_{r1} r_1(T_1, C_{A1}, C_{B1})}{\sum_i^{A,B,C,D} C_{i1} C_{pi} V_1} + \frac{-\Delta H_{r2} r_2(T_1, C_{B1}, C_{C1})}{\sum_i^{A,B,C,D} C_{i1} C_{pi} V_1} \quad (1e)$$

$$\frac{dC_{A2}}{dt} = \frac{F_3 C_{A1} - F_5 C_{A2}}{V_2} - r_1(T_2, C_{A2}, C_{B2}) \quad (1f)$$

$$\frac{dC_{B2}}{dt} = \frac{F_3 C_{B1} + F_4 C_{B0} - F_5 C_{B2}}{V_2} - r_1(T_2, C_{A2}, C_{B2}) - r_2(T_2, C_{B2}, C_{C2}) \quad (1g)$$

$$\frac{dC_{C2}}{dt} = \frac{F_3 C_{C1} - F_5 C_{C2}}{V_2} + r_1(T_2, C_{A2}, C_{B2}) - r_2(T_2, C_{B2}, C_{C2}) \quad (1h)$$

$$\frac{dC_{D2}}{dt} = \frac{F_3 C_{D1} - F_5 C_{R2}}{V_2} + r_2(T_2, C_{B2}, C_{C2}) \quad (1i)$$

$$\frac{dT_2}{dt} = \frac{Q_2 + F_4 C_{B0} H_B(T_{B0})}{\sum_i^{A,B,C,D} C_{i2} C_{pi} V_2} + \frac{\sum_i^{A,B,C,D} (F_3 C_{i1} H_i(T_1) - F_5 C_{i2} H_i(T_2))}{\sum_i^{A,B,C,D} C_{i2} C_{pi} V_2} + \frac{-\Delta H_{r1} r_1(T_2, C_{A2}, C_{B2})}{\sum_i^{A,B,C,D} C_{i2} C_{pi} V_2} + \frac{-\Delta H_{r2} r_2(T_2, C_{A2}, C_{B2})}{\sum_i^{A,B,C,D} C_{i2} C_{pi} V_2} \quad (1j)$$

$$\frac{dC_{A3}}{dt} = \frac{F_5 C_{A2} - F_7 C_{A3}}{V_3} - r_1(T_3, C_{A3}, C_{B3}) \quad (1k)$$

$$\frac{dC_{B3}}{dt} = \frac{F_5 C_{B2} + F_6 C_{B0} - F_7 C_{B3}}{V_3} - r_1(T_3, C_{A3}, C_{B3}) - r_2(T_3, C_{B3}, C_{C3}) \quad (1l)$$

$$\frac{dC_{C3}}{dt} = \frac{F_5 C_{C2} - F_7 C_{C3}}{V_3} + r_1(T_3, C_{A3}, C_{B3}) - r_2(T_3, C_{B3}, C_{C3}) \quad (1m)$$

$$\frac{dC_{D3}}{dt} = \frac{F_5 C_{D2} - F_7 C_{D3}}{V_3} + r_2(T_3, C_{B3}, C_{C3}) \quad (1n)$$

$$\frac{dT_3}{dt} = \frac{Q_3 + F_6 C_{B0} H_B(T_{B0})}{\sum_i^{A,B,C,D} C_{i3} C_{pi} V_3} + \frac{\sum_i^{A,B,C,D} (F_5 C_{i2} H_i(T_2) - F_7 C_{i3} H_i(T_3))}{\sum_i^{A,B,C,D} C_{i3} C_{pi} V_3} + \frac{-\Delta H_{r1} r_1(T_3, C_{A3}, C_{B3})}{\sum_i^{A,B,C,D} C_{i3} C_{pi} V_3} + \frac{-\Delta H_{r2} r_2(T_3, C_{B3}, C_{C3})}{\sum_i^{A,B,C,D} C_{i3} C_{pi} V_3} \quad (1o)$$

$$\frac{dC_{A4}}{dt} = \frac{F_7 C_{A3} + F_9 C_{A5} - F_r C_{Ar} - F_8 C_{A4}}{V_4} \quad (1p)$$

$$\frac{dC_{B4}}{dt} = \frac{F_7 C_{B3} + F_9 C_{B5} - F_r C_{Br} - F_8 C_{B4}}{V_4} \quad (1q)$$

$$\frac{dC_{C4}}{dt} = \frac{F_7 C_{C3} + F_9 C_{C5} - F_r C_{Cr} - F_8 C_{C4}}{V_4} \quad (1r)$$

$$\frac{dC_{D4}}{dt} = \frac{F_7 C_{D3} + F_9 C_{D5} - F_r C_{Dr} - F_8 C_{D4}}{V_4} \quad (1s)$$

$$\frac{dT_4}{dt} = \frac{Q_4 + \sum_i^{A,B,C,D} (F_7 C_{i3} H_i(T_3) + F_9 C_{i5} H_i(T_5))}{\sum_i^{A,B,C,D} C_{i4} C_{pi} V_4} - \frac{(F_r C_{ir} H_i(T_4) + F_8 C_{i4} H_i(T_4)}{\sum_i^{A,B,C,D} C_{i4} C_{pi} V_4} - \frac{F_r C_{ir} H_{vapi})}{\sum_i^{A,B,C,D} C_{i4} C_{pi} V_4} \quad (1t)$$

$$\frac{dC_{A5}}{dt} = \frac{F_{r1} C_{Ar} - F_9 C_{A5}}{V_5} - r_3(T_5, C_{A5}, C_{D5}) \quad (1u)$$

$$\frac{dC_{B5}}{dt} = \frac{F_{r1} C_{Br} - F_9 C_{B5}}{V_5} - r_2(T_5, C_{B5}, C_{C5}) \quad (1v)$$

$$\frac{dC_{C5}}{dt} = \frac{F_{r1} C_{Cr} - F_9 C_{C5}}{V_5} - r_2(T_5, C_{B5}, C_{C5}) + 2r_3(T_5, C_{A5}, C_{D5}) \quad (1w)$$

$$\frac{dC_{D5}}{dt} = \frac{F_{r1} C_{Dr} + F_{10} C_{D0} - F_9 C_{D5}}{V_5} + r_2(T_5, C_{B5}, C_{C5}) - r_3(T_5, C_{A5}, C_{D5}) \quad (1x)$$

$$\frac{dT_5}{dt} = \frac{Q_5 + F_{10} C_{D0} H_D(T_{D0})}{\sum_i^{A,B,C,D} C_{i5} C_{pi} V_5} + \frac{\sum_i^{A,B,C,D} (F_r C_{ir} H_i(T_4) - F_9 C_{i5} H_i(T_5))}{\sum_i^{A,B,C,D} C_{i5} C_{pi} V_5} + \frac{-\Delta H_{r2} r_2(T_5, C_{B5}, C_{C5})}{\sum_i^{A,B,C,D} C_{i5} C_{pi} V_5} + \frac{-\Delta H_{r3} r_3(T_5, C_{A5}, C_{D5})}{\sum_i^{A,B,C,D} C_{i5} C_{pi} V_5} \quad (1y)$$

In the process model of Eq. 1, r_1, r_2 and r_3 are the reaction rates of reactions 1, 2 and 3 respectively and H_i, $i = A,\ B,\ C,\ D$, are the enthalpies of the reactants. The reaction rates are related to the concentrations of the reactants and the temperature in each reactor as follows:

$$r_1(T, C_A, C_B) = k_{r1} C_A^{0.32} C_B^{1.5},$$

$$r_2(T, C_B, C_C) = \frac{k_{r2} C_B^{2.5} C_C^{0.5}}{(1 + k_{EB2} C_D)},$$

$$r_3(T, C_A, C_D) = \frac{k_{r3} C_A^{1.0218} C_D}{(1 + k_{EB3} C_A)}$$

with

$$k_{r1} = 0.0840e^{(-9502/RT)},\ k_{r2} = 0.0850e^{(-20640/RT)},$$
$$k_{r3} = 237.8e^{(-61280/RT)},\ k_{EB2} = 0.0152e^{(-3933/RT)},$$
$$k_{EB3} = 0.4901e^{(-50870/RT)}.$$

The heat capacities of the species are assumed to be constants and the molar enthalpies have a linear dependence on temperature as follows:

$$H_i(T) = H_{iref} + C_{pi}(T - T_{ref})$$

where C_{pi}, $i = A,\ B,\ C,\ D$ are heat capacities.

The model of the flash tank separator is developed under the assumption that the relative volatility of each species has a linear correlation with the temperature of the vessel within the operating temperature range of the flash tank, as shown below:

$$\begin{array}{rclcrcl} \alpha_A &=& 0.0449T_4 + 10, & \quad & \alpha_B &=& 0.0260T_4 + 10 \\ \alpha_C &=& 0.0065T_4 + 0.5, & & \alpha_D &=& 0.0058T_4 + 0.25 \end{array}$$

where α_i, $i = A,\ B,\ C, D$, represent the relative volatilities. It has also been assumed that there is a negligible amount of reaction taking place in the separator. The following algebraic equations model the composition of the overhead stream relative to the composition of the liquid holdup in the flash tank:

$$M_i = (F_7 C_{i3} + F_9 C_{i5}) \frac{\alpha_i (F_7 C_{i3} + F_9 C_{i5})}{\sum_{k}^{A,B,C,D} \alpha_k (F_7 C_{k3} + F_9 C_{k5})}$$

where M_i, $i = A,\ B,\ C,\ D$ are the molar flow rates of the overhead reactants. Based on M_i, $i = A,\ B,\ C,\ D$, we can calculate the concentration of the reactants in the recycle streams as follows:

$$C_{ir} = \frac{M_i}{\sum_{k}^{A,B,C,D} M_i / C_{k0}}, \quad i = A, B, C, D$$

where C_{k0}, $k = A, B, C, D$, are the mole densities of pure reactants. The condensation of vapor takes place overhead, and a portion of the condensed liquid is purged back to separator to keep the flow rate of the recycle stream at a fixed value. The temperature of the condensed liquid is assumed to be the same as the temperature of the vessel.

The definitions for the variables used in the above model can be found in Table I, with the parameter values given in Table II.

Each of the tanks has an external heat/coolant input. The manipulated inputs to the process are the heat injected to or removed from the five vessels, Q_1, Q_2, Q_3, Q_4 and Q_5, and the feed stream flow rates to CSTR-2 and CSTR-3, F_4 and F_6.

The states of the process consist of the concentrations of A, B, C, D in each of the five vessels and the temperatures of the vessels. They are assumed to be available continuously to the controllers. We consider a stable steady state (operating point), x_s, of the process which is defined by the steady-state inputs Q_{1s}, Q_{2s}, Q_{3s}, Q_{4s}, Q_{5s}, F_{4s} and F_{6s}, as shown in Table III. The steady-state values of the temperatures in the five vessels are the following:

$$T_{1s} = 477.24\ K,\ T_{2s} = 476.97\ K,\ T_{3s} = 473.47\ K,$$
$$T_{4s} = 470.60\ K,\ T_{5s} = 478.28\ K.$$

TABLE I

PROCESS VARIABLES

C_{A1}, C_{B1}, C_{C1}, C_{D1}	Concentrations of $A,\ B,\ C,\ D$ in CSTR-1
C_{A2}, C_{B2}, C_{C2} ,C_{D2}	Concentrations of $A,\ B,\ C,\ D$ in CSTR-2
C_{A3}, C_{B3}, C_{C3}, C_{D3}	Concentrations of $A,\ B,\ C,\ D$ in CSTR-3
C_{A4}, C_{B4}, C_{C4}, C_{D4}	Concentrations of $A,\ B,\ C,\ D$ in separator
C_{A5}, C_{B5}, C_{C5}, C_{D5}	Concentrations of $A,\ B,\ C,\ D$ in CSTR-4
C_{Ar}, C_{Br}, C_{Cr}, C_{Dr}	Concentrations of $A,\ B,\ C,\ D$ in F_r
T_1, T_2, T_3, T_4, T_5	Temperatures in each vessel
T_ref	Reference temperature
F_3, F_5, F_7, F_8, F_9	Effluent flow rates from each vessel
F_1, F_2, F_4, F_6, F_10	Feed flow rates to each vessel
F_r, F_{r1}, F_{r2}	Recycle flow rates
H_{vapA}, H_{vapB}	Enthalpies of vaporization of $A,\ B$
H_{vapC}, H_{vapD}	Enthalpies of vaporization of $C,\ D$
H_{Aref}, H_{Bref}	Enthalpies of $A,\ B$ at T_{ref}
H_{Cref}, H_{Dref}	Enthalpies of $C,\ D$ at T_{ref}
ΔH_{r1}, ΔH_{r2}, ΔH_{r3}	Heat of reactions 1, 2 and 3
V_1, V_2, V_3, V_4, V_5	Volume of each vessel
Q_1, Q_2, Q_3, Q_4, Q_5	External heat/coolant inputs to each vessel
C_{pA}, C_{pB}, C_{pC}, C_{pD}	Heat capacity of $A,\ B,\ C,\ D$
α_A, α_B, α_C, α_D	Relative volatilities of $A,\ B,\ C,\ D$
C_{A0}, C_{B0}, C_{C0}, C_{D0}	Molar densities of pure $A,\ B,\ C,\ D$
T_{A0}, T_{B0}, T_{D0}	Feed temperatures of pure $A,\ B,\ D$

TABLE II

PARAMETER VALUES

$F_1 = 7.1 \times 10^{-3}$	m^3/s	$F_r = 0.012$	m^3/s
$F_2 = 8.697 \times 10^{-4}$	m^3/s	$F_{r1} = 0.006$	m^3/s
$F_{r2} = 0.006$	m^3/s	$V_1 = 1$	m^3
$F_10 = 2.31 \times 10^{-3}$	m^3/s	$V_2 = 1$	m^3
$H_{vapA} = 3.073 \times 10^4$	$J/mole$	$V_3 = 1$	m^3
$H_{vapB} = 1.35 \times 10^4$	$J/mole$	$V_4 = 3$	m^3
$H_{vapC} = 4.226 \times 10^4$	$J/mole$	$V_5 = 1$	m^3
$H_{vapD} = 4.55 \times 10^4$	$J/mole$	$C_{pA} = 184.6$	$J/mole \cdot K$
$\Delta H_{r1} = -1.536 \times 10^5$	$J/mole$	$C_{pB} = 59.1$	$J/mole \cdot K$
$\Delta H_{r2} = -1.118 \times 10^5$	$J/mole$	$C_{pC} = 247$	$J/mole \cdot K$
$\Delta H_{r3} = 4.141 \times 10^5$	$J/mole$	$C_{pD} = 301.3$	$J/mole \cdot K$
$C_{A0} = 1.126 \times 10^4$	$mole/m^3$	$T_{ref} = 450$	K
$C_{B0} = 2.028 \times 10^4$	$mole/m^3$	$T_{A0} = 473$	K
$C_{C0} = 8174$	$mole/m^3$	$T_{B0} = 473$	K
$C_{D0} = 6485$	$mole/m^3$	$T_{D0} = 473$	K

II. DESIGN OF DISTRIBUTED MODEL PREDICTIVE CONTROLLERS

In this section, we will first construct a Lyapunov-based controller which can stabilize the closed-loop process asymptotically; and then we will construct a centralized Lyapunov-based model predictive control (LMPC) design and two

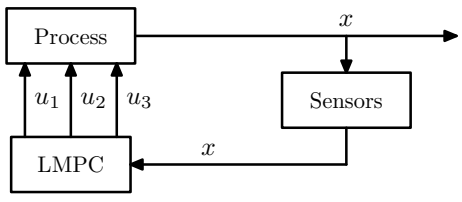

Fig. 2. Centralized LMPC.

TABLE III

STEADY-STATE INPUT VALUES FOR x_s.

Q_{1s}	4.4×10^6 $[J/s]$	Q_{2s}	4.6×10^6 $[J/s]$
Q_{3s}	4.7×10^6 $[J/s]$	Q_{4s}	9.2×10^6 $[J/s]$
Q_{5s}	5.9×10^6 $[J/s]$	$F_{4s},\ F_{6s}$	8.697×10^{-4} $[m^3/s]$

TABLE IV

MANIPULATED INPUT CONSTRAINTS.

$\lvert u_{11}\rvert \le 7.5\times10^5\ [J/s]$	$\lvert u_{1i}\rvert \le 5\times10^5\ [J/s], (i=2,3)$
$\lvert u_{21}\rvert \le 6\times10^5\ [J/s]$	$\lvert u_{22}\rvert \le 5\times10^5\ [J/s]$
$\lvert u_{31}\rvert \le 4.93\times10^{-5}\ [m^3/s]$	$\lvert u_{32}\rvert \le 4.93\times10^{-5}\ [m^3/s]$

distributed model predictive control (DMPC) designs based on the Lyapunov-based controller. Specifically, the centralized LMPC is based on the LMPC proposed in [8], [9] which guarantees practical stability of the closed-loop system, allows for an explicit characterization of the stability region. The two DMPC schemes are proposed in [1]. One of them adopts a one-directional communication network and its distributed controllers are designed via LMPC techniques, evaluated in sequence and once at each sampling time. This DMPC design will be termed as sequential DMPC below. The other DMPC scheme utilizes a bi-directional communication network and its distributed controllers are also designed via LMPC techniques; they are evaluated in parallel and iterate to improve closed-loop performance. This design will be termed as iterative DMPC below.

The control objective is to regulate the system from an initial state to the steady state. The first distributed controller (LMPC 1) is designed to compute the values of Q_1, Q_2 and Q_3, the second distributed controller (LMPC 2) is designed to compute the values of Q_4 and Q_5, and the third distributed controller (LMPC 3) is designed to compute the values of F_4 and F_6. Taking these into account, the process model of Eq. 1 belongs to the following class of nonlinear systems:

$$\dot{x}(t) = f(x) + g_1(x)u_1(x) + g_2(x)u_2(x) + g_3(x)u_3(x)$$

where the state x is the deviation of the state of the process from the steady state, $u_1^T = [u_{11}\ u_{12}\ u_{13}] = [Q_1 - Q_{1s}\ Q_{2s}\ Q_3 - Q_{3s}]$, $u_2^T = [u_{21}\ u_{22}] = [Q_4 - Q_{4s}\ Q_5 - Q_{5s}]$ and $u_3^T = [u_{31}\ u_{32}] = [F_4 - F_{4s}\ F_6 - F_{6s}]$ are the manipulated inputs which are subject to the constraints shown in Table IV.

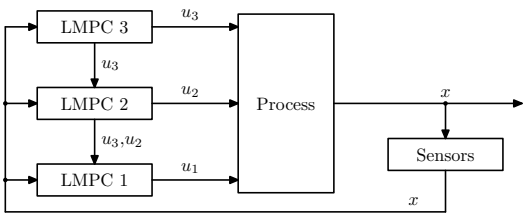

Fig. 3. Sequential DMPC.

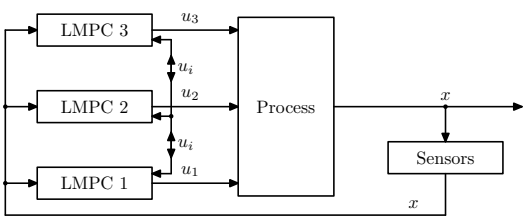

Fig. 4. Iterative DMPC.

In the centralized LMPC scheme, the centralized LMPC optimizes the values of u_1, u_2 and u_3 in a single optimization problem as shown in Fig. 2. In the DMPC schemes, one LMPC is assigned to each manipulated input. In the sequential DMPC scheme, the distributed controllers communicate in one-directional manner as shown in Fig. 3. Specifically, LMPC 3 sends its future input to LMPC 2 and LMPC 2 sends its and LMPC 3's future input to LMPC 1. In the iterative DMPC scheme, each distributed controller is able to communicate to all the other controllers as shown in Fig. 4. Specifically, LMPC 1, LMPC 2 and LMPC 3 can exchange future input information before each iteration, and they can iterate to improve the closed-loop performance.

In the control of the process, u_1 and u_2 are necessary to keep the stability of the closed-loop system, while u_3 can be used as an extra manipulated input to improve the closed-loop performance. We first construct the Lyapunov-based controller $h(x) = [h_1(x)\ h_2(x)\ h_3(x)]^T$. Specifically, $h_1(x)$ and $h_2(x)$ are designed as follows [7]:

$$h_i(x) = \begin{cases} -\frac{L_fV + \sqrt{(L_fV)^2 + (L_{g_i}V)^4}}{(L_{g_i}V)^2} L_{g_i}V & \text{if } L_{g_i}V \neq 0 \\ 0 & \text{if } L_{g_i}V = 0 \end{cases}$$

where $i = 1,\ 2$, $L_fV = \dfrac{\partial V}{\partial x} f(x)$ and $L_{g_i}V = \dfrac{\partial V}{\partial x} g_i(x)$ denote the Lie derivatives of the scalar function V with respect to the vector fields f and g_i ($i = 1,\ 2$), respectively. The controller $h_3(x)$ is chosen to be $h_3(x) = [0\ 0]^T$ because the input set u_3 is not needed to stabilize the process. In the simulations, we consider a quadratic Lyapunov function $V(x) = x^T P x$ with P being the following weighting matrix:

$$P = diag^*(P_v).$$

where $P_v = [1\ 1\ 1\ 1\ 10\ 1\ 1\ 1\ 1\ 10\ 1\ 1\ 1\ 1\ 10\ 1\ 1\ 1\ 1\ 10\ 1\ 1\ 1\ 1\ 10]$. The weights in P are chosen by a trail-and-error procedure. The basic idea behind this procedure is that more weight should be put on the temperatures of the five vessels because temperatures have more significant effect on the overall control performance, and the Lyapunov-based controller $h(x)$ should be able to stabilize the closed-loop system asymptotically with continuous feedback and actuation.

Based on $h(x)$, we design the centralized LMPC, the sequential distributed LMPC and the iterative distributed LMPC. The sampling time used is $\Delta = 30\ s$ and the weighting matrices

$$Q_c = diag(Q_v)$$

where $Q_v = [1\ 1\ 1\ 1\ 10^3\ 1\ 1\ 1\ 1\ 10^3\ 10\ 10\ 10\ 10\ 10^4\ 1\ 1\ 1\ 1\ 10^3\ 1\ 1\ 1\ 1\ 10^3]$ and $R_{c1} = diag([10^{-8}\ 10^{-8}\ 10^{-8}])$, $R_{c2} = diag([10^{-8}\ 10^{-8}])$ and $R_{c3} = diag([1\ 1])$.

$^*diag(v)$ denotes a matrix with its diagonal elements being the elements of vector v and all the other elements being zeros.

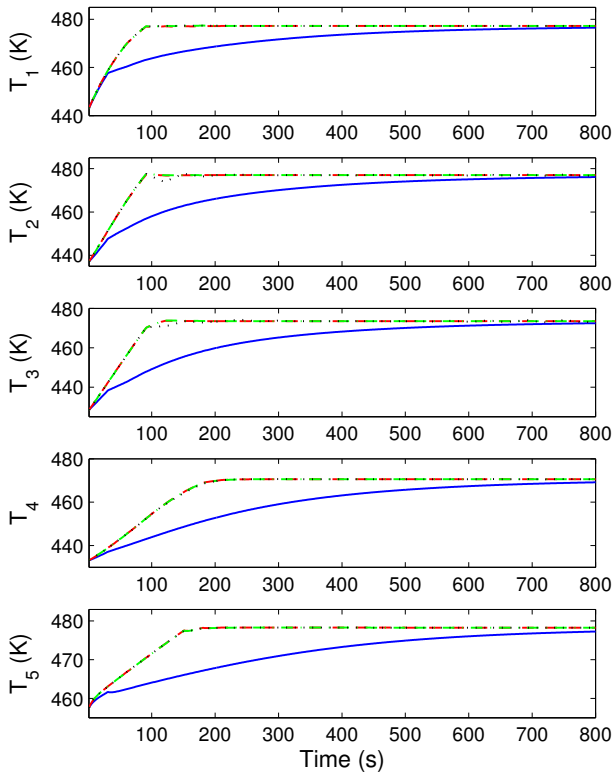

Fig. 5. Trajectories of temperatures under the Lyapunov-based controller $h(x)$ (solid line), the centralized LMPC (dashed line), the sequential DMPC (dash-dotted line) and the iterative DMPC with $c = 1$ (dotted line).

III. Simulation results

First, we carried out a set of simulations to demonstrate that the Lyapunov-based controller and the different control designs can all drive the state of the process to the required steady-state. Figure 5 shows the trajectories of the temperatures in the five vessels. From the figure, we can see that the centralized LMPC, the sequential and iterative LMPCs give similar temperature trajectories and enforce the convergence of the states to the desired steady-state much faster than the trajectories under the Lyapunov-based controller $h(x)$. All the concentration trajectories in the five vessels display similar convergence trends of the temperature trajectories. We omit the figures of the concentration trajectories here due to space limitations.

In order to illustrate the asymptotical convergence of the state of the closed-loop process under different control schemes, we also show the trajectories of the Lyapunov function $V(x)$ under the different control schemes in Fig 6. Note that because of the stability constraints in the formulations of the sequential, iterative DMPCs and the centralized LMPC (see [8], [9], [1] for the designs of these LMPCs), the trajectories of $V(x)$ under the centralized LMPC, the sequential DMPC and the iterative DMPC are bounded by the corresponding trajectory of $V(x)$ under the Lyapunov-based controller $h(x)$.

Next, we compare the mean evaluation times of the

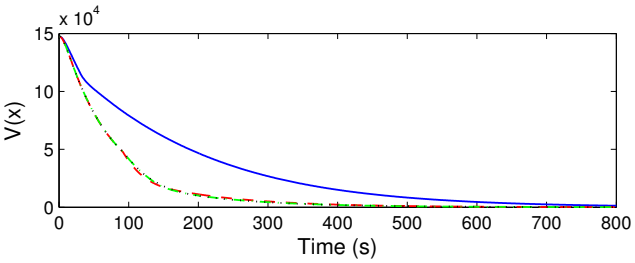

Fig. 6. Trajectories of the Lyapunov function $V(x)$ under the Lyapunov-based controller $h(x)$ (solid line), the centralized LMPC (dashed line), the sequential DMPC (dash-dotted line) and the iterative DMPC with $c = 1$ (dotted line).

TABLE V

Mean evaluation time of different LMPC optimization problems for 100 evaluations.

		$N = 1$ (s)	$N = 3$ (s)	$N = 6$ (s)
Centralized LMPC		2.192	8.694	27.890
Sequential	LMPC 1	0.472	2.358	6.515
	LMPC 2	0.497	1.700	4.493
	LMPC 3	0.365	1.453	3.991
Iterative	LMPC 1	0.484	2.371	6.280
	LMPC 2	0.426	1.716	4.413
	LMPC 3	0.185	0.854	2.355

centralized LMPC optimization problem with the mean evaluation times of the LMPC optimization problems in the sequential and iterative DMPCs. Each LMPC optimization problem was evaluated 100 times at different conditions. Different prediction horizons were considered in this set of simulations. The simulations were carried out using Java programming language in a Pentium 3.20 GHz computer. The optimization problems were solved by the open source interior point optimizer Ipopt [10]. The results are shown in Table V. We can see that for different prediction horizons, the time needed to solve the optimization problems of the centralized LMPC is much larger than the time needed to solve the optimization problems in the sequential or iterative DMPC. This is because the centralized LMPC has to solve a much larger (in terms of decision variables) optimization problem than the ones of the distributed LMPCs. Another observation from the table is that the evaluation time of the centralized LMPC is larger than the sum of evaluation times of LMPC 1, LMPC 2 and LMPC 3 of the sequential DMPC, and the times needed to solve the distributed LMPCs in both sequential and iterative distributed schemes are of the same order of magnitude.

In another set of simulations, we compare the centralized LMPC and the two DMPC schemes from a performance index point of view. The prediction horizon for this set of simulations is $N = 1$. To carry out the comparison, the same initial condition and parameters are used for the different control schemes and the total cost index under each control scheme is computed as follows:

$$\begin{aligned} J &= \sum_{i=0}^{M} (x(t_i)^T Q_c x(t_i) + u_1(t_i)^T R_{c1} u_1(t_i)) \\ &\quad + \sum_{i=0}^{M} (u_2(t_i)^T R_{c2} u_2(t_i) + u_3(t_i)^T R_{c3} u_3(t_i)) \end{aligned}$$

TABLE VI

TOTAL PERFORMANCE COST ALONG THE CLOSED-LOOP SYSTEM TRAJECTORIES I.

	J ($\times 10^7$)			
Centralized	1.8858			
Sequential	1.8891			
	$c=1$	$c=3$	$c=5$	$c=7$
Iterative	1.8955	1.8883	1.8867	1.8863
	$c=9$	$c=11$	$c=13$	$c=15$
	1.8862	1.8859	1.8858	1.8858

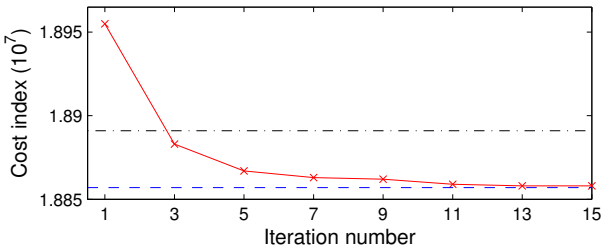

Fig. 7. Total performance cost along the closed-loop system trajectories of centralized LMPC (dashed line), sequential distributed LMPC (dash-dotted line) and iterative distributed LMPC (solid line).

where $t_0 = 0$ is the initial time of the simulations, $t_i = t_0 + i\Delta$ are the time instants taken into account and $t_M = 1000\ s$ is the end of the simulations. Table VI shows the total cost along the closed-loop system trajectories under the different control schemes. In this set of simulations, the centralized LMPC gives the lowest performance cost, the sequential DMPC gives lower cost than the iterative DMPC when there is no iteration ($c = 1$). However, as the iteration number c increases, the performance cost given by the iterative DMPC decreases and converges to the cost of the one corresponding to the centralized LMPC. This point is also shown in Fig. 7.

Note that the above set of simulations only represents one possible case. As we discussed in Remarks 11-12 in [1], there is no guaranteed convergence of the performance of distributed MPC to the performance of a centralized MPC, and there is also no guaranteed superiority of the performance of one DMPC scheme over the others. Specifically, we show another two sets of simulations to illustrate these points. In both sets of simulations, we chose different matrices R_{c1} and R_{c2}, and all the other parameters (Q_c, R_{c3}, Δ, N) remained the same as the previous set of simulations. In the first set of simulations, we picked $R_{c1} = diag([5\times10^{-5}\ 5\times10^{-5}\ 5\times10^{-5}])$, $R_{c2} = diag([5\times10^{-5}\ 5\times10^{-5}])$ and the results are shown in Table VII. It shows that the centralized LMPC provides a much lower cost than the ones of both the sequential and iterative DMPCs. We can also see that as the number of iterations increases, the iterative distributed LMPC converges to a value which is different from the one obtained by the centralized LMPC. In the second set of simulations, we picked $R_{c1} = diag([1\times10^{-4}\ 1\times10^{-4}\ 1\times10^{-4}])$, $R_{c2} = diag([1\times10^{-4}\ 1\times10^{-4}])$ and the results are shown in Table VIII, from which we can see that the centralized LMPC provides a higher cost than the ones of both DMPCs.

TABLE VII

TOTAL PERFORMANCE COST ALONG THE CLOSED-LOOP SYSTEM TRAJECTORIES II.

	J ($\times 10^7$)			
Centralized	5.052			
Sequential	7.039			
	$c=1$	$c=3$	$c=5$	$c=6$
Iterative	7.2286	7.2241	7.2240	7.2240

TABLE VIII

TOTAL PERFORMANCE COST ALONG THE CLOSED-LOOP SYSTEM TRAJECTORIES III.

	J ($\times 10^7$)		
Centralized	3.8564		
Sequential	3.6755		
	$c=1$	$c=3$	$c=4$
Iterative	3.6663	3.6639	3.6639

IV. CONCLUSIONS

In this work, we focused on the application of the theoretical results of DMPC architectures developed in [1] to a catalytic alkylation of benzene process example which consists of four continuous stirred tank reactors (CSTRs) and a flash separator. First principle model developed via mass and energy balances was used to carry out simulations. Three separate Lyapunov-based model predictive controllers were designed to control the process in a coordinative fashion. Extensive simulations were carried out to compare the proposed DMPC architectures with existing centralized LMPC techniques from computational time and closed-loop performance points of view.

REFERENCES

[1] J. Liu, X. Chen, D. Muñoz de la Peña, and P. D. Christofides, "Sequential and iterative architectures for distributed model predictive control of nonlinear process systems. Part I: theory," *Proceedings of 2010 American Control Conference*, in press.

[2] H. Ganji, J. Ahari, A. Farshi, and M. Kakavand, "Modelling and simulation of benzene alkylation process reactors for production of ethylbenzene," *Petroleum and Coal*, vol. 46, pp. 55–63, 2004.

[3] W. J. Lee, "Ethylbenzene dehydrogenation into styrene: kinetic modeling and reactor simulation," Ph.D. dissertation, Texas A&M University, College Station, TX, 2005.

[4] C. Perego and P. Ingallina, "Combining alkylation and transalkylation for alkylaromatic production," *Green Chemistry*, vol. 6, pp. 274–279, 2004.

[5] G. B. Woodle, *Ethylbenzene*. New York: Taylor & Francis Group, 2006, vol. I, ch. Petrochemicals and Petrochemical Processing, pp. 929–941.

[6] H. You, W. Long, and Y. Pan, "The mechanism and kinetics for the alkylation of benzene with ethylene," *Petroleum Science and Technology*, vol. 24, pp. 1079–1088, 2006.

[7] E. Sontag, "A 'universal' construction of Artstein's theorem on nonlinear stabilization," *Systems and Control Letters*, vol. 13, no. 13, pp. 117–123, 1989.

[8] P. Mhaskar, N. H. El-Farra, and P. D. Christofides, "Predictive control of switched nonlinear systems with scheduled mode transitions," *IEEE Transactions on Automatic Control*, vol. 50, pp. 1670–1680, 2005.

[9] P. Mhaskar, N. H. El-Farra, and P. D. Christofides, "Stabilization of nonlinear systems with state and control constraints using Lyapunov-based predictive control," *Systems and Control Letters*, vol. 55, pp. 650–659, 2006.

[10] A. Wächter and L. T. Biegler, "On the implementation of primal-dual interior point filter line search algorithm for large-scale nonlinear programming," *Mathematical Programming*, vol. 106, pp. 25–57, 2006.